arXiv:1212.6052v1 [physics.flu-dyn] 25 Dec 2012

What happens to turbulent skin-friction drag reduction at high Re?

Davide Gatti[1] and Maurizio Quadrio[2]
[1] *Center of Smart Interfaces, TU Darmstadt, Petersenstr. 32, 64287 Darmstadt, Germany*[a)]
[2] *Dept. Aerospace Sciences and Technologies, Politecnico di Milano, Via La Masa 34, 20156 Milano, Italy*[b)]

(Dated: 27 December 2012)

We address one of the capital problems in the field of turbulent skin-friction drag reduction, i.e. the performance of the known techniques at high values of the Reynolds number Re. We limit ourselves to considering open-loop techniques based on spanwise forcing (oscillating wall, streamwise-travelling waves), and explore via Direct Numerical Simulations (DNS) how quickly the drag reduction and net energy savings decrease when the friction Reynolds number is increased. We consider turbulent channel flow up to $Re_\tau = 2000$. Owing to the demanding computational cost of large-scale simulations, the size of the computational domain in the homogeneous directions is reduced while keeping under control the statistical uncertainty related to the finite time average. This allows us to carry out a full parametric study (at least at $Re_\tau = 1000$), hence avoiding the two assumptions that the low-Re optimum set of parameters remains optimal at higher Re, and that the optimum obeys an inner scaling.

Although this computational strategy definitely decreases the absolute fidelity of the DNS results, a careful estimation of the errors allows us to interpret the obtained results by suggesting an unexpected and interesting scenario where the performance of the drag-reduction technique degrade with Re with a markedly different rate depending on the parameters. In particular, the known optimal region turns out to be such at low-Re only, since there drag reduction degrades quite fast with Re, in line with available results. However, other regions are much less sensitive to Re, or insensitive at all. If one considers that the energy required to create the forcing presents a slightly favorable trend with Re, the possibility exists of net energy saving at very high Reynolds numbers.

This interesting scenario remains speculative in nature, owing to the spatial truncation implied by the limited domain size. However, a few full-scale DNS for the traveling waves at $Re_\tau = 400$ have been carried out, and their results fully support the suggested scenario, which, though appealing, would force us to rethink our current understanding of how these drag reduction techniques work and behave at high Re.

Keywords: Turbulent skin-friction drag reduction, DNS, high Reynolds number

I. INTRODUCTION

Decreasing the aerodynamic drag in the turbulent regime is a technological objective that is prompting the study and development of several techniques aimed at skin-friction drag reduction, being the increase of friction drag above the laminar value one of the fundamental manifestations of turbulence in the simplest wall-bounded flow. The techniques under development possess a wide range of effectiveness, ranging from passive techniques (a classic example being riblets[12]) that yield up 8–10% drag reduction in well controlled, low-Reynolds laboratory conditions, to active techniques based on linear control theory[20] that promise much better performance, especially in terms of net energy savings, but are characterized by high complexity and have been studied through high-fidelity Direct Numerical Simulations (DNS). Midway between these two extrema, open-loop active techniques compromise between energy gain and energy expenditure to yield sizable net energy savings with the advantage of moderate complexity, as they do not require the deployment of micron-sized sensors and only require relatively large-scale actuators. One recently proposed strategy, that looks promising in terms of net energy saving potential, is the streamwise-traveling waves concept[28], that has been shown to provide at least 20% net energy savings and has been already given experimental verification[1]. The long-term perspectives of these drag reduction techniques are illustrated in a recent volume devoted to the subject[21].

[a)] Electronic mail: gatti@csi.tu-darmstadt.de
[b)] Electronic mail: maurizio.quadrio@polimi.it

Besides the obvious need for further technological development of sensors and actuators, essentially all the active techniques lack a thorough evaluation in flows characterized by high values of the Reynolds number. Unfortunately, however, most of the anticipated applications are at high Re. In this paper we critically address the effect of varying the Reynolds number on wall-based open-loop control techniques by focusing on one particular control strategy: the streamwise-traveling waves of spanwise wall velocity

$$W(x,t) = A\cos\left(\frac{2\pi}{\lambda_x}x - \frac{2\pi}{T}t\right)$$

where $W(x,t)$ is the velocity forcing at the wall, of amplitude A. This forcing law contains the two cases of the spanwise-oscillating wall, for $\lambda_x \to \infty$, and the steady wave when $\omega = 0$.

It is the present Authors' opinion that this is becoming the most fundamental question that should be answered in this research field. The reason why few data exist at high Re are quite obvious, and can be traced back to the enormous increase of the computational cost of DNS for increasing Re, paralleled by a shrinking of the physical size of the required sensors and actuators to be employed in an experiment. Using wall-based strategies to affect the turbulence wall cycle, that was shown to be autonomous[17], does not guarantee that performances scale up at high Re, and in fact the few available data, covering less than one decade in Re, witness a significant decrease of, for example, maximum drag reduction. It remains to be understood whether such a decrease is a low-Re effect, so that performances are deemed to stabilize as soon as Re becomes large enough, or is expected to continue indefinitely, so that the level of zero drag reduction is reached at values of Re which are still smaller than those typical of applications. Figure 1 graphically illustrates the two scenarios and shows that both are compatible with the available low-Re numerical and laboratory experiments, so that it can not be inferred which one is more likely to occur. The only information available is the result of the study by Iwamoto et al[14], who used both analytical developments and DNS experiments to show that a virtual drag reduction technique capable of removing near-wall turbulent fluctuations in a turbulent plane channel flow for $y^+ < 10$ still yields 35% drag reduction at the relatively large value of $Re_\tau = 10^5$.

We are unaware of studies where the spanwise-traveling waves by Du & Karniadakis[9] have been studied as a function of the Reynolds number. For the present class of techniques, the available information on the high-Re behavior is as follows. J.I.Choi et al[4] used turbulent channel flow simulations at $Re_\tau = 100, 200$ and 400 to suggest that, at $T^+ = 100$ and $A^+ = 10$, the oscillating wall produces a drag reduction of 41.1%, 29.9% and 22.4% at the three Reynolds numbers respectively. They fitted their results with those available in the literature to infer that the drag reduction is predictable by a quadratic function of a scaling parameter V_c that is proportional to $Re_\tau^{-0.2}$. The finding is coherent with the results reported above that show a $Re_\tau^{-0.4}$ dependency. Ricco & Quadrio[30] reported that the spanwise-oscillating wall at $T^+ = 125$ and $A^+ = 12$ yields 32.5% drag reduction at $Re_\tau = 200$ and 28.1% at $Re_\tau = 400$. Compared to the results of J.I.Choi et al[4], a slower decay against Re is obtained, of only $Re_\tau^{-0.2}$, probably owing to the differences in the forcing parameters and in the numerical discretization, being the resolution higher in the latter case. Quadrio, Ricco & Viotti[28] determined the best-performing traveling wave at $Re_\tau = 200$ and forcing intensity of $A^+ = 12$, and verified that at $Re_\tau = 400$ maximum drag reduction decreases from 48% to 42%, again supposing a power law dependency, R would decrease as $Re_\tau^{-0.19}$. Touber & Leschziner[33] present DNS data at $Re_\tau = 200, 500$ as well as LES and one DNS datapoint at $Re_\tau = 1000$ to propose that drag reduction values obtained under similar values of a scaling parameter S decrease roughly as $Re_\tau^{-0.2}$, thus confirming the findings of J.I.Choi et al[4]. Lockerby et al[10] presented a linear stability study to investigate the influence of a spanwise generalized Stokes' layer on the growth of near-wall turbulent streaks. The streak amplification is shown to be strictly related to the drag reduction predicted by numerical experiments, suggesting the importance of basic linear mechanisms on the drag reduction. Their linearized model allows predictions at higher Reynolds number, and the effect of the Reynolds number is found to be much milder than that obtained in simulations. In a recent paper by Moarref & Jovanović[23], a model-based approach that employs linearized Navier-Stokes equations in conjunction with turbulence modeling is developed. The Re-effect up to $Re_\tau = 934$ is addressed for the spanwise-oscillating wall: the optimal frequency of oscillation is found to increase with Re, and the drag reduction decreases as $Re_\tau^{-0.15}$, i.e. again at a slightly slower yet still comparable rate than numerical experiments. If exception is made for the last two works, that span a parameter range but are limited by their inherent uncertainty, all the others tracked only the neighborhood of the forcing parameters yielding maximum drag reduction at low Re, for the oscillating wall case, on the assumption that these optimum forcing conditions scale in wall units. We are unaware of laboratory experiments that have been able to significantly vary the value of Re. Although it is true that experiments are typically carried out at values of Re which are somewhat higher than those typical of DNS (typically

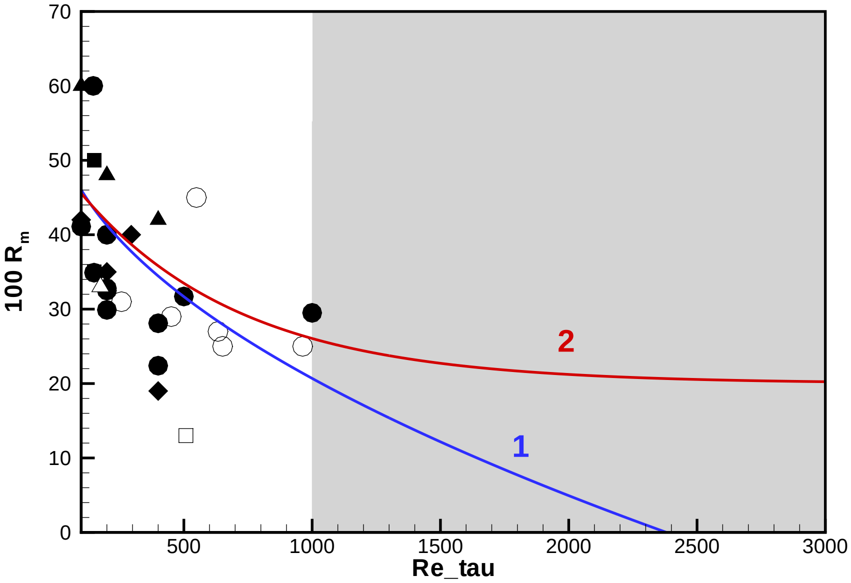

FIG. 1. Variation with Re of maximum drag reduction R_{max} for spanwise forcing as educed from several studies. Black symbols indicate numerical (DNS) studies, and open symbols are for experimental studies. We explicitly note that the forcing amplitude is not always comparable among different datasets. Circles: oscillating wall[4–6,18,24,27,29–34]; triangles: streamwise-travelling waves[1,28]; squares: spanwise-travelling waves[8,9]; triangles: Lorentz force[3,25]. The gray area marks the ”unknown zone” where drag reduction could drop according to one of the two lines drawn in the sketch, i.e. falling rapidly to zero (blue line, scenario 1) or gradually decreasing the drop rate (red line, scenario 2).

$Re_\tau = 600$), experimental uncertainty, and above all the issue of the spatial transient that makes a control surface only partially effective precludes putting together numerical and experimental data to precisely assess trends of DR reduction with Re based on mixed datasets.

In this paper, we use DNS to obtain information on the performance of the spanwise-oscillating wall and the streamwise-traveling waves up to $Re_\tau = 2000$, using DNS. The aim is to be able to carry out a parametric study at higher Re, so as to avoid the double hypothesis implicitly assumed in the previous works. In fact it has traditionally been assumed that at low-Re optimal parameters determined at low Re remain optimal at higher Re, assuming they scale in wall units. To keep the computational study manageable, our strategy is one of changing the size of the computational domain while carefully controlling the effect of this essential discretization parameter on the reliability of the obtained drag reduction information. On one hand, random and systematic errors may be introduced and are rigorously estimated. On the other, the simplified framework of a narrower domain can give useful suggestive results on the behavior of drag reduction and on the importance of the truncated large turbulent scales on it.

The structure of the paper is as follows. Firstly the numerical strategy and simulation parameters are described in detail, focusing on the eventual convenience of using a reduced domain, on the strategy we adopted to estimate random errors on the mean skin-friction. The parameters needed to evaluate the control are described as well before estimating the influences of a smaller domain on the skin-friction of the uncontrolled and controlled channel-flow. In the third section the drag reduction ratio for traveling-waves up to $Re_\tau = 2000$ is discussed and the so-called Re-effect quantified. In the fourth section interesting insights on the power consumption and power budget are given, followed by concluding remarks.

Re_p	Case	L_z/h	L_x/h	L_z^+	L_x^+	$n_x \times n_y \times n_z$	$\langle \mathrm{d}u/\mathrm{d}y \rangle$	Re_τ
4760	Ref1	2.5	5	497	993	$96 \times 100 \times 96$	8.29	198
	ChA	1.67	3.3	333	665	$64 \times 100 \times 64$	8.37	200
	ChB	3.33	6.67	663	1326	$128 \times 100 \times 128$	8.31	199
	ChC	5	10	997	1994	$192 \times 100 \times 192$	8.36	199
	Ref2	**3.14**	**6.28**	**625**	**1250**	$\mathbf{128 \times 100 \times 128}$	**8.32**	**199**
29500	Ref1	0.5	1	459	918	$96 \times 500 \times 96$	28.54	917
	Ref2	**0.66**	**1.32**	**627**	**1255**	$\mathbf{128 \times 500 \times 128}$	**30.63**	**951**
	ChA	0.68	1.36	644	1288	$128 \times 500 \times 128$	30.41	947
	ChB	0.35	0.7	303	606	$64 \times 500 \times 64$	26.5	868
	ChC	1.98	0.99	969	1938	$192 \times 500 \times 12$	32.6	980
73000	**Ref1**	**0.63**	**1.28**	**1339**	**2678**	$\mathbf{192 \times 1000 \times 192}$	**60.18**	**2096**

TABLE I. Computational domain size and friction Reynolds number Re_τ.

II. METHOD

A. Code and simulation parameters

The analysis is carried out on a newly created DNS dataset. The computer code used for the calculations, its parallel algorithm and the architecture of the computing system have been described elsewhere[22]. The code is a mixed-discretization parallel solver of the incompressible Navier–Stokes equations, based on Fourier expansions in the homogeneous directions and high-order explicit compact finite-difference schemes in the wall-normal direction. Most of the calculations have been run on a computing system available in dedicated mode at the Università di Salerno. If exception is made for the domain size, discussed below, there is nothing specific about the present set of calculations. The governing equations are integrated forward in time, starting from an initial condition of fully developed uncontrolled channel flow, generated specifically for each Reynolds number. The flow rate is kept constant and the bulk velocity is $U_b = 2/3U_p$, where U_p is the centerline velocity of a Poiseuille flow with the same flow rate. Parametric DNS studies have been carried out at $Re_p = U_p h/\nu = 4760$ and 23500, corresponding to $Re_\tau = u_\tau h/\nu = 200$ and 1000 respectively, based on the friction velocity u_τ of the unmanipulated flow. A more limited dataset is produced at $Re_p = 73000$, corresponding to $Re_\tau = 2000$, the highest Reynolds number reached during this investigation.

The spatial resolution in the stream- and spanwise directions is $\Delta x^+ = 10$ and $\Delta z^+ = 5$, the wall-normal resolution varies from $\Delta y^+_{min} = 1$ at the wall to $\Delta y^+_{max} = 6.9$ at the centerline, with the number of grid points in this directions set at $Re_\tau/2$. The resolution has been kept constant in wall units while varying the Reynolds number. In all of the traveling-wave calculations at $Re_\tau = 200$ and $Re_\tau = 1000$ the streamwise length was set to $L_x^+ = 1250$ wall units, while the spanwise length was $L_z^+ = 625$. The domain size has been increased to $L_x^+ = 2700$ and $L_z^+ = 1350$ at $Re_\tau = 2000$ to improve the reliability of the results. We note that such domains are of reduced sizes compared to the computational domains that are customarily employed but are still rather large when compared to the Minimal Flow Unit[16], the smallest domain that can self-sustain turbulence. The domain used for the oscillating wall (Ref1 in table I) is slighly smaller, being $L_x^+ = 2L_z^+ \approx 1000$. As figure 2 shows, the domains used for all the traveling-wave cases are only three times smaller in width and length, compared to a typical domain used in channel flow simulations, while they are still 20 times bigger than the minimal domain. The domain sizes used for most of the simulations at each Reynolds number are shown in bold in table I, together with other domain dimensions that have been simulated to run the size-sensitivity tests discussed below.

These box sizes are the result of an accurate *a posteriori* study to find the best compromise among accuracy, reliability and computational efficiency. Nonetheless, the following *a priori* criteria identify a bound for the domain extent required to represent the drag reduction phenomenon reasonably well.

First of all, the domain should be large enough to avoid any obviously nonphysical narrow-channel effect, such as one-sided turbulence[16]. This basic requirement is always amply verified in our simulations. Next, all the turbulent structures that affect the wall shear and are thus potentially involved in the drag reduction should be present, but this is a more stringent requirement as well as more difficult to be clearly stated. Although the periodic boundary conditions imply an in(de)finite spatial domain, choosing the fundamental wavenumbers in the horizontal directions sets an upper limit for the structures that fit into the domain. In the near-wall region, the size of the turbulent structures increases with the distance from the wall. By increasing the distance form the wall, the box width or length may become too small, so that the size of

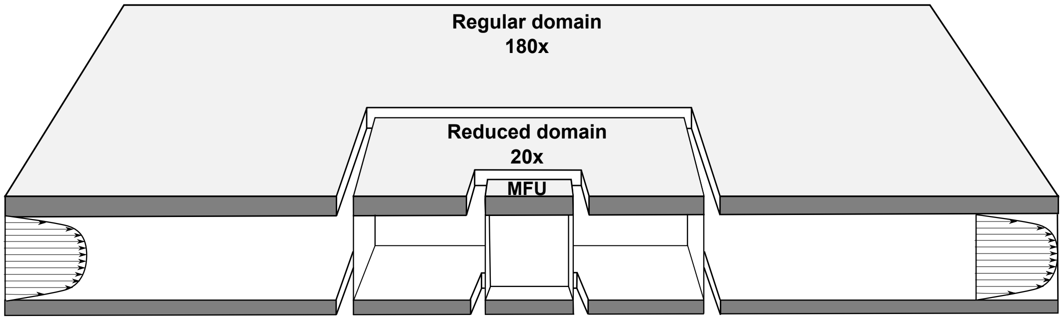

FIG. 2. Size of a regular domain compared to the reduced domain used in his work and the Minimal Flow Unit presented by Jiménez and Moin[16].

the structures is constrained loosing its dependency on the wall distance. Based on the aspect-ratio of the most common near-wall turbulent structures, the turbulence will be well-resolved up to a distance y_d from the wall if the spanwise length $L_z^+ \approx 3y_d^+$[11]. The final requirement on L_z is found by considering that the logarithmic region has to be well resolved to obtain good prediction of the wall shear[11].

The streamwise length of the computational box has been dictated by the fundamental wavelength λ_x of the wall forcing, or by the will to keep an $x-z$ aspect ratio of 2:1. In any case, the minimal limit[11] for a good description of the logarithmic layer $L_x^+ \approx h^+$ has been respected.

A real benefit is obtained by the use of reduced domain when the averaging time is adjusted, so that a slight uncertainty on the wall shear prediction is still allowed. This will keep under control the simulation time and hence the computational cost. After various attempts, simulations were run for a time equal to $T_{sim}U_p/h = 1500$ at $Re_\tau = 200$, in viscous timescale $T_{sim}^+ = 12500$. At $Re_\tau = 1000$ simulation time has been kept constant in viscous unit, leading to a simulation time $T_{sim}U_p/h = 400$. As a result, the uncertainty level on wall shear is increased, because both the actual averaging area and integration time in outer units are reduced. At $Re_\tau = 2000$ a time of $T_{sim}U_p/h = 400$ has been used, resulting in $T_{sim}^+ = 24000$, in order to increase the reliability of the results.

The control parameters are chosen such as to to compare present results to those presented by Quadrio et al[28]. In particular, $A^+ = 12$ is chosen, although this is not the optimal choice to study the net power. For clarity sake we report in figure 3 the drag reduction ratio results by Quadrio et al[28] accompanied by five dashed lines marking the regions of the parameter space investigated in the present work. Two scans at constant wavenumber have been made, one for the oscillating wall case at $\kappa_x = 0$ (line 1) and one at $\kappa_x^+ = 0.005$, corresponding to $\lambda_x^+ = 1250$ (line 2). Here, more full channel DNS data are available and the maximum DR is achieved at low-Re. Two more sweeps at constant frequency $\omega^+ = -0.2$ (line 3) and $\omega^+ = 0.012$ (line 4) have been done to study the effect of a change in wavelength. Several waves on the locus of maximum DR, at constant wavespeed $c^+ = 2.5$, are also considered (line 5). A wide region of the parameter space is then spanned. The maximum frequency and wavenumber analyzed are equal, in wall units, to those of Quadrio et al.[28].

B. Computational cost

The existence of a long initial transient during the onset of statistically-steady drag-reduction is a peculiar feature to the present problem that makes the run of parametric studies particularly expensive. Its duration does not depend on the domain size and for a full DNS it usually takes a significant part of the computational effort only to get rid of the initial transient. This is crucial when trying to achieve a full parametric study of an open-loop flow-control technique.

The simulation of smaller domains clearly reduces the time needed to advance the simulation by one time step and thus the time spent in resolving the transient. The per-timestep computational cost due to the pseudo-spectral convolutions can be expressed, following Jiménez[15], as $Q \sim N_y N_x N_z \log(N_x N_z)$, where N_x, N_y and N_z are the number of modes/collocation points in the three directions. If we consider a domain aspect ratio of $L_x/L_z = 2/1$ and a resolution $\Delta x^+ = 2\Delta z^+ = 10$, the number of modes in the homogeneous direction is $N_x = N_z = L_x^+/\Delta x^+$. It follows that the time required to advance a timestep is more than 16 times shorter if a domain box that is four times shorter and narrower than a regular domain is used.

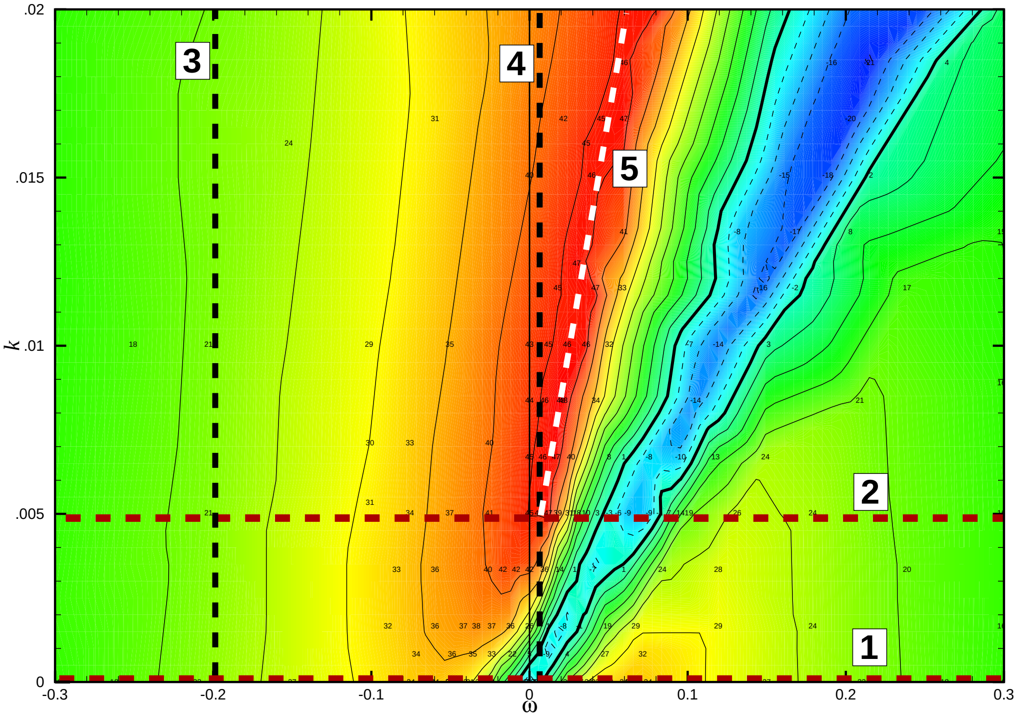

FIG. 3. Map of the drag reduction ratio 100R versus the wavenumber κ_x and frequency ω of the traveling wave at $A^+ = 12$ and $Re_\tau = 200$, after Quadrio et al[28]. The dashed lines represent the portions of the parameters space investigated in this work. Dark red: constant κ_x simulations; black: constant ω simulations; white: constant c simulations.

If on one hand the wall-clock time needed to reach a statistically-steady flow is shortened, on the other hand with a restricted domain the averaging time needs to be larger than 10 wash-outs to still yield "good" statistics, i.e. statistics with the same uncertainty level (of course here we are neglecting any possible narrow-channel effect). The standard deviation of the mean wall-shear can be expressed as:

$$\sigma_{\overline{\tau}} \sim \sigma_\tau / \sqrt{T_{\text{sim}}} \tag{1}$$

where σ_τ is the standard deviation of the spatially-averaged wall-shear signal that is proportional to $(\mathcal{A}^+)^{-1/2}$, where $\mathcal{A} = L_x \times L_z$ is the area of the domain. This means that a 16 times smaller domain would require a 16 times longer average to keep the same uncertainty level. It is then clear that an advantage can be achieved with a smaller domain mainly if the domain size is decreased while keeping a finite averaging time. We allowed then for a certain value of uncertainty on the measured skin-friction that clearly needs to be estimated in terms of confidence interval in order to have a meaningful result.

C. Random uncertainty evaluation

A strategy is needed to estimate the uncertainty on the measured drag reduction ratio R that involves only the time-resolved data of the space-averaged wall-shear stress τ. When a finite averaging-time is used in combination with a domain of reduced size, σ_τ increases while T_{sim} is finite, so that the uncertainty on the mean due to the intrinsic randomness of the process may not be negligible.

The method used in this work is based on the assumption that statistical data are single realizations, equally spaced in time, of a continuous stationary (ergodic) random processes. Strong stationarity specifies that all statistical moments are time-invariant. Implicit in this is also the assumption that the signals are free from any initial transient. Under these hypotheses, the standard deviation of the mean $\sigma_{\overline{\tau}}$ is related to the autocorrelation function $\rho(\Delta t)$ as follows:

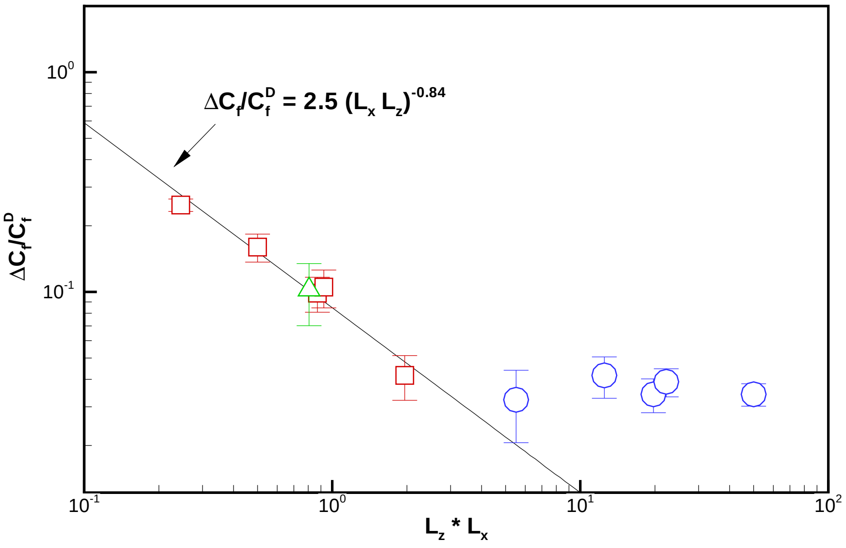

FIG. 4. Values of the friction coefficient C_f versus the size L_xL_z of the computational domain expressed in wall units. Horizontal lines are the values of C_f as educed from the Dean correlation.

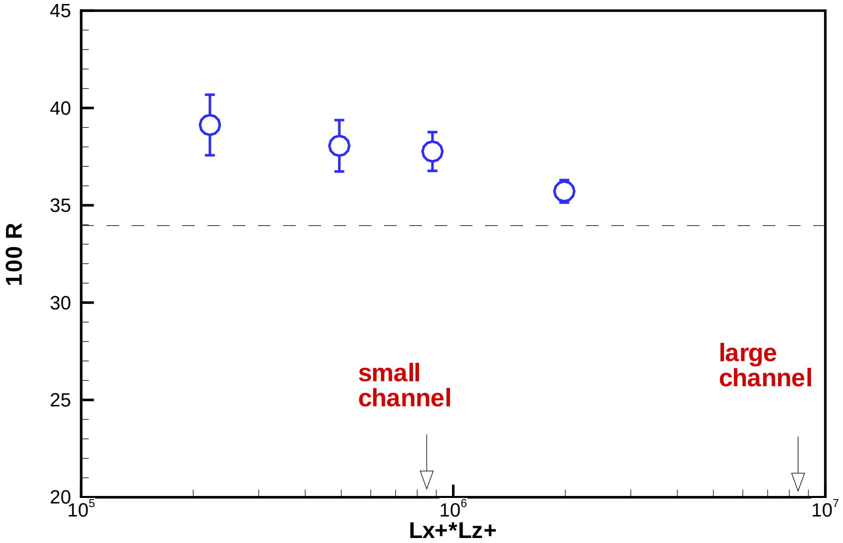

FIG. 5. Values of the drag reduction $100R$ achieved with the oscillating wall, at $Re_\tau = 200$, $T^+ = 125$ and $A^+ = 12$, versus the size of the computational domain expressed in wall units. The horizontal line marks the value computed by DNS in Quadrio & Ricco[27].

$$\sigma_{\overline{\tau}}^2 = \frac{2\sigma_\tau^2}{T_{\text{sim}}} \int_0^{T_{\text{sim}}} \rho(\Delta t) \left(1 - \frac{|\Delta t|}{T_{\text{sim}}}\right) \mathrm{d}\Delta t$$

where $\rho(\Delta t) = \mathrm{E}[\tau(t)\tau(t+\Delta t)]/\sigma_\tau^2$ and $\mathrm{E}[\cdot]$ is the expected value operator. When $T_{\text{sim}} \gg \Delta t_{\max}$, then the expression reduces to $\sigma_{\overline{\tau}} = 2(\sigma_\tau^2/T_{\text{sim}})\mathcal{T}$, where $\mathcal{T} = \int_0^{T_{\text{sim}}} \rho(\Delta t)\mathrm{d}\Delta t$ is the integral timescale of the process.

The timescale accounts for the need to discard data points in the time-resolved history that can not be considered uncorrelated. The variance of the wall shear and the autocovariance involved in the definition of autocorrelation are themselves unknown and can not be measured directly, therefore their best estimators, the sample standard deviation squared s_τ^2 and the sample covariance $q(\Delta t)$, are used instead.

The standard uncertainty of the drag reduction ratio s_R is computed by propagating via RSS the sample standard deviation of the mean skin-friction of both the uncontrolled $s_{\overline{\tau}0}$ and the controlled $s_{\overline{\tau}}$ case. A confidence interval for R can be obtained thanks to the central limit theorem, hence:

$$\mathrm{R} - \gamma s_\mathrm{R} \leq \mu_\mathrm{R} \leq \mathrm{R} + \gamma s_\mathrm{R}$$

where $\gamma = z_{\alpha/2}$ is the standardized confidence interval of a normalized Gaussian PDF and depends on the desired confidence level $1 - \alpha$. In this work the common confidence level of 0.95 has been chosen.

D. Parameters for control evaluation

The control performances are evaluated through the three dimensionless parameters introduced by Kasagi et al.[19], (R, P_{in} and S), that describe the total energy budget. The time-averaged pumping power per channel wall area is defined as:

$$P = \frac{U_b}{T_\mathrm{sim} - T_i} \int_{T_i}^{T_\mathrm{sim}} < \tau_x > \, \mathrm{d}t$$

where τ_x denotes the streamwise component of the wall-shear stress and $< \cdot >$ is the wall space-average operator. The reduction of the pumping power due to the control is then

$$R = \frac{P_0 - P}{P_0}$$

where P and P_0 are the pumping powers required to drive the controlled and reference flow respectively. It is important to notice that in a constant flow-rate simulation the reduction of the pumping power is identically equal to the reduction of the skin-friction drag. The power introduced into the system to apply the control is the input power per unit area P_{in}, defied as the power needed to drive the wall against the spanwise wall-shear:

$$P_{in} = \frac{1}{P_0 \left(T_\mathrm{sim} - T_i\right)} \int_{T_i}^{T_\mathrm{sim}} < W \tau_z > \, \mathrm{d}t \tag{2}$$

where τ_z is the spanwise component of the wall-shear stress. The budget between benefits and costs of the control can be then easily defined as:

$$S = R - P_{in}$$

E. Narrow-channel effects

The use of smaller domains brings about a potential bias in the flow statistic and, in particular, in the mean skin-friction coefficients. It turns out that the skin-friction is increasingly underestimated for decreasing domain sizes. The effect is evident in figure 4: the relative error between the computed C_f and that predicted by the Dean's[7] correlation C_f^D is shown against the domain size in outer units. A deterministic behavior is found and in this range of Re an empiric power-law holds between the relative error and the domain area. At the larger domain sizes used at $Re_\tau = 200$ the trend of the relative error is shaded by the statistical error and by the known slight inaccuracy of the Dean's correlation at low Re. The domain size at Re_τ 1000 and 2000 has always been chosen to have a relative error of less than 10%.

The drag reduction ratio is itself affected by a change in the domain size. Even though at $Re_\tau = 200$ the mean skin-friction coefficient of the uncontrolled channel is almost insensitive to a reduction of domain area, figure 5 shows that the narrower the domain, the larger the drag reduction ratio. Within the uncertainty the behavior is almost linear and is most probably due to a combination of a virtually further reduced domain size in viscous units in case of high DR, bringing along an underestimation of C_f, as well as to a more

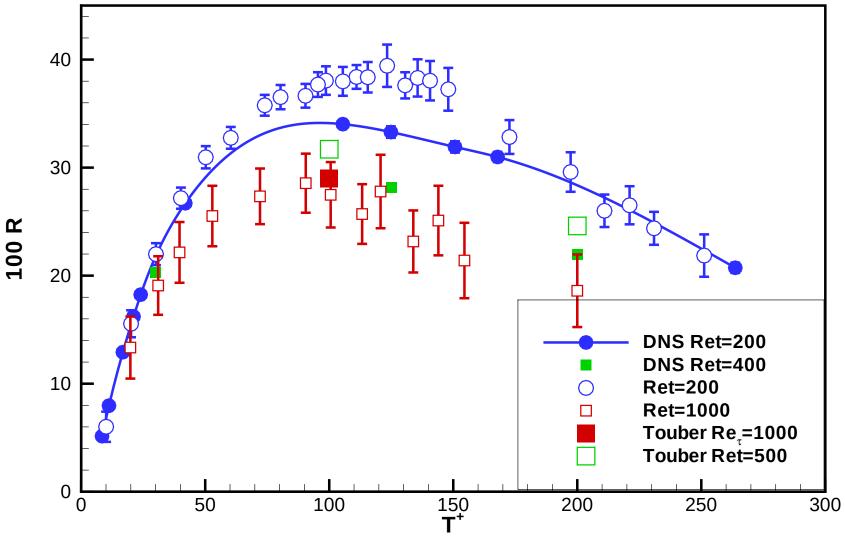

FIG. 6. Percentage drag reduction $100R$ versus oscillation period T^+ for the oscillating wall, at $A^+ = 12$. Blu open circles: $Re_\tau = 200$; red open squares: $Re_\tau = 1000$. Error bars at 95% confidence level. Reference DNS data: blu solid line and filled circles, $Re_\tau = 200$ from[27]; filled green squares, $Re_\tau = 400$ from[30]; open green squares: $Re_\tau = 500$ from[33]; closed red square: $Re_\tau = 1000$ from[33].

ordered structure of turbulence, prone to be affected by the control. The latter is both a drawback and a potential strength of the method, which could give a more comprehensible picture of the drag reduction mechanism, by discarding part of the turbulent structure that do not directly participate in the autonomous regeneration cycle and offering a more ordered array of elemental turbulent structures. Nevertheless, it is important to point out that the reported case of figure 5 is in the region of the parameter space that is mostly affected by this effect. When traveling waves are employed and, in general, when the drag reduction is below 0.3, this effect is not observed.

III. DRAG REDUCTION RATIO

Figure 6 represents the drag reduction ratio R for a wall oscillating with a non-dimensional period T^+. Here and throughout the rest of the paper our new direct numerical simulation are presented as big empty colored symbols. Color and shape refer to different values of the Reynolds number: blue circles at $Re_\tau = 200$, red squares at $Re_\tau = 1000$ and green triangles at $Re_\tau = 2000$. Error bars have been added to the presently computed data, for the 95% of confidence level. (The error bars are not seen when their size is within the marker). Literature data at different Re are drawn with other colors and specified in the legend. Our data are superimposed to well-established, low-Re, DNS datasets represented as filled circles, in particular those at $Re_\tau = 200$ by Quadrio and Ricco[27] and those at $Re_\tau = 400$ by Ricco and Quadrio[30] for the oscillating wall ($\kappa_x = 0$), and those at $Re_\tau = 200$ by Quadrio et al.[28] for the traveling waves. When available, higher-Re simulations are reported: here those at $Re_\tau = 500$ and $Re_\tau = 1000$ by Touber and Leschziner[33].

The already available DNS data span a significant part of the parameter space only at the low Reynolds number of $Re_\tau = 200$, while the more recently computed data points at higher values of Reynolds number sample the parameter space more sparsely and focus only on the optimal period $T^+ \approx 125$ or on its neighborhood.

We observe that the values of R obtained with the present simulations at $Re_\tau = 200$ agree very well with those obtained with full-channel simulations in Quadrio and Ricco[27] at the same Reynolds number. The agreement is perfect at values of T^+ much larger and much smaller than the optimum value. Near the optimum, though the position of the maximum is well-captured, a slight overestimation of the drag reduction occurs, together with an increase of the uncertainty. This overestimation decreases to only 1%

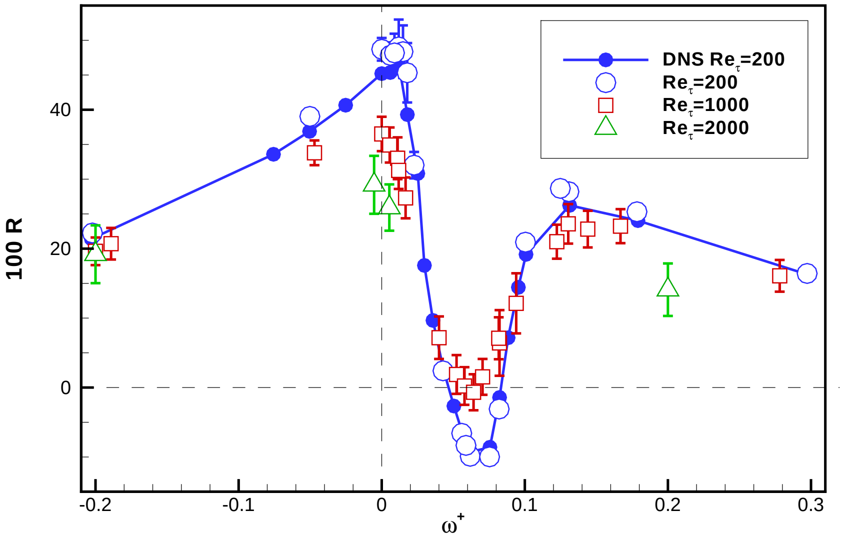

FIG. 7. Percentage drag reduction ratio $100R$ versus oscillating frequency ω^+ for the streamwise-travelling waves, at $A^+ = 12$ and $\lambda^+ = 1250$. Blu open circles: $Re_\tau = 200$; red open squares: $Re_\tau = 1000$; green open triangles: $Re_\tau = 2000$. Error bars at 95% confidence level. Reference DNS data: blu solid line and filled circles, $Re_\tau = 200$ from[28].

for the traveling waves. In the followings reference full-channel DNS are reported to confirm the very good agreement with present simulations at low Re that will not be underlined again. It is interesting to point out the agreement with the point taken from Touber and Leschziner[33] at $Re_\tau = 1000$, though it lies on slightly bigger value of DR. The curious overestimation of Touber's data is even more evident at $Re_\tau = 500$: their point at $T^+ = 200$ has an higher DR than the point obtained via full-channel DNS at $Re_\tau = 400$.

When the Reynolds is increased to $Re_\tau = 1000$ our dataset shows that the maximum drag reduction ratio consequently reduces from 0.39 to 0.29, and occurs at $T^+ = 90$, thus the data are consistent with a shift of the optimal period towards lesser values. The shift is a result of the unevenly sensitivity to Re throughout the whole range of T^+. In particular, as suggested by Ricco and Quadrio[30], the decrease appears to be much less significant at low values of T^+, while it is amplified at high T^+. As a result a similar DR is achieved at $T^+ = 50$ and $T^+ = 100$.

This scenario of heterogeneous dependence of R upon Re is fully confirmed if we enlarge to the κ_x^+-ω^+ plane of the traveling waves at Re_τ up to 2000. Figure 7 plots $100R$ for the horizontal slice numbered (2) in figure 3: i.e. as a function of the forcing frequency ω^+ for waves with constant wavelength $\lambda^+ = 1250$. The maximum drag reduction ratio achieved at this Re is very high and equal to 0.49, while the reference data provide $R = 0.48$, with a difference clearly within the confidence interval.

As the Reynolds number is increased to $Re_\tau = 1000$, R$_{max}$ drops to 0.37, with a total loss of 0.12. A similarly significant change can be observed in the "valley" of R, where at low Re the waves produce a negative R, i.e. a drag increase. Although the drag increase almost disappears, the minimum of R is still present and seems to widen, embracing a larger range of ω^+. Again, the data suggest that the optimal value of the control parameters might change with Re. At this wavelength, the optimal point is the standing wave, $\omega^+ = 0$, at higher Re. As in the previously discussed case of the oscillating wall, the most important observation that can be drawn from the figure is that the influence of Re is heterogeneous over the parameter space, being stronger approaching the region of DI. Outside of this region, and in particular for $|\omega^+| > 0.15$, R remains nearly unchanged.

The dataset at $Re_\tau = 2000$ consists of four points only that indeed confirm the general trend discussed above: the DI valley is widening and influencing the neighborhoods. It pushes high-DR regions on its right toward higher frequencies and on its left toward lower frequencies. The highest DR on the slice is $R = 0.29$, at $\omega = -0.05$.

In figure 8, the interest is focused on the low-Re ridge of maximum R, i.e. the locus of points with

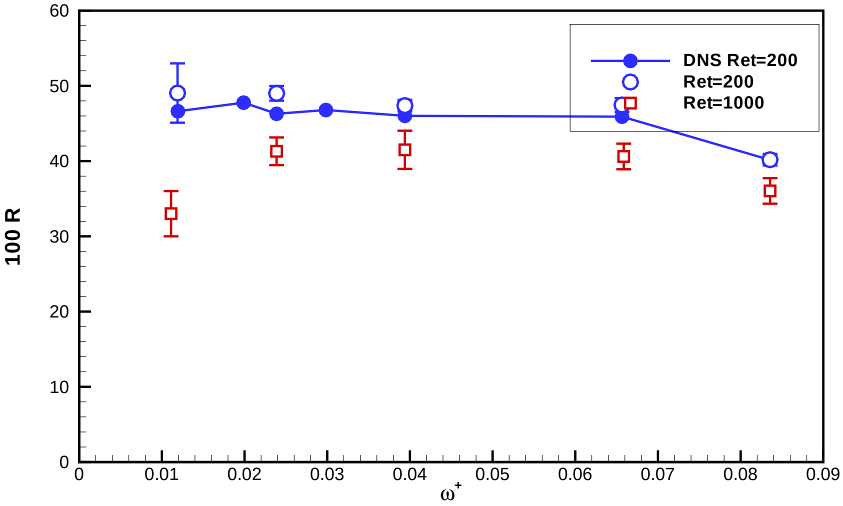

FIG. 8. Percentage drag reduction $100R$ versus the oscillating frequency ω^+ for the streamwise-travelling waves, at $A^+ = 12$ and along the ridge of the low-Re maximum, defined as $c^+ = 2.5$. Symbols as in figure 7.

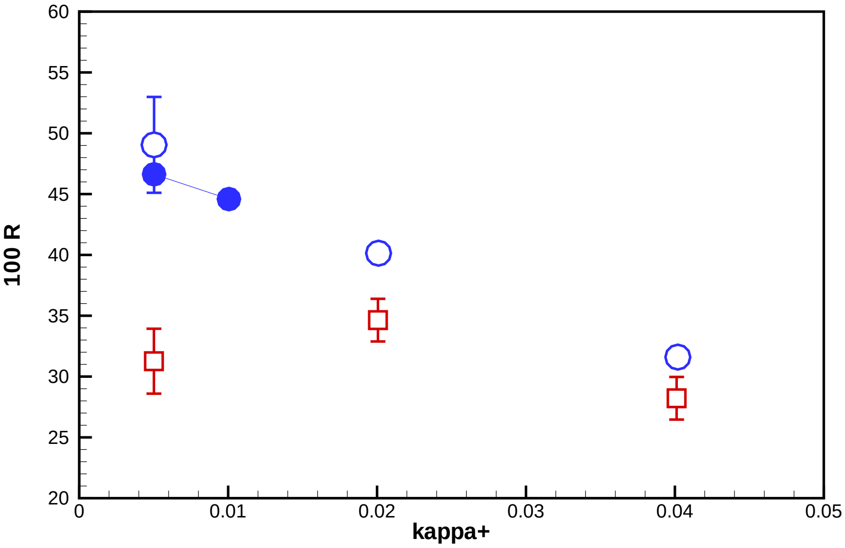

FIG. 9. Percentage drag reduction 100R versus the wavenumber κ_x^+ for the streamwise-travelling waves, at $A^+ = 12$ and $\omega^+ = 0.012$. Symbols as in figure 7.

maximum R that approximately extends along the line $c^+ \approx 2.5$ (line (3) in figure 3). The low-frequency low-wavenumber ('southern') region of the ridge is particularly affected by a change in Re while the right high-frequency part is almost insensitive: here we encountered at $Re_\tau = 1000$ the maximum R of 0.42. The DR ridge seems to be moving upwards or, in other words, its 'southern' low-κ_x^+ tail is receding.

This scenario is fully confirmed by the two further constant-ω^+ sections of the $\kappa - \omega$ plane, namely at $\omega^+ = 0.012$ and $\omega^+ = -0.2$, shown in figure 9 and 10 respectively. From the first the receding behavior of the low-wavenumber part of the ridge is extremely evident: at $\kappa^+ = 0.005$ the DR almost halves by increasing Re_τ to 1000. In the latter the trend of R towards higher wavenumbers is milder but still present,

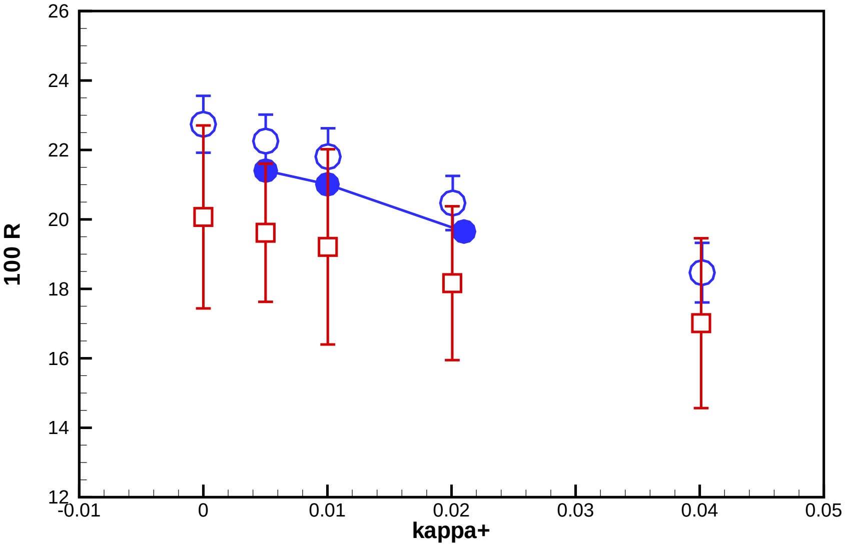

FIG. 10. Percentage drag reduction $100R$ versus the wavenumber κ_x^+ for the streamwise-travelling waves, at $A^+ = 12$ and $\omega^+ = -0.2$.

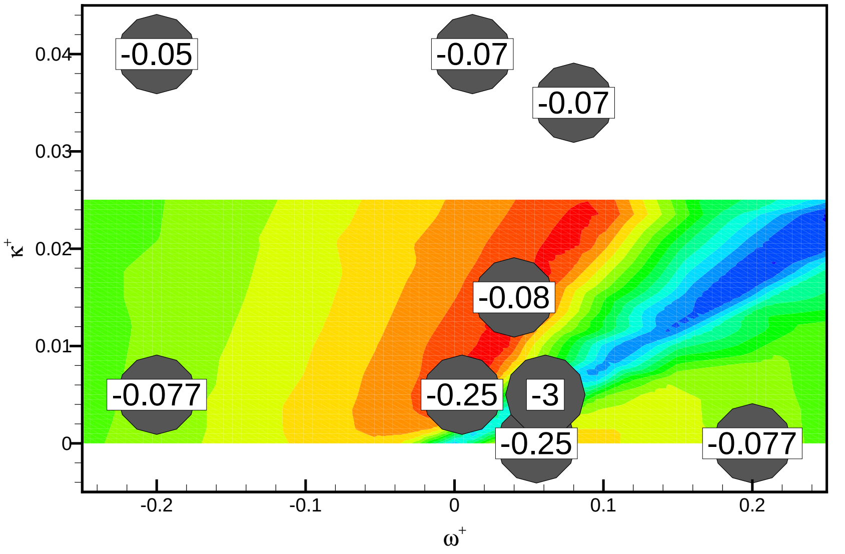

FIG. 11. In the filled circles the value of the Reynolds sensitivity exponent γ, supposing R $\sim Re_\tau^\gamma$ superimposed to the drag reduction map after[28].

though shaded by the large confidence interval.

A. Dependence upon Re

To quantify the Re-sensitivity, now and in the following we will adopt the usual supposition that in the present Reynolds number range R is proportional to Re_τ^γ. This common choice is rather arbitrary and based

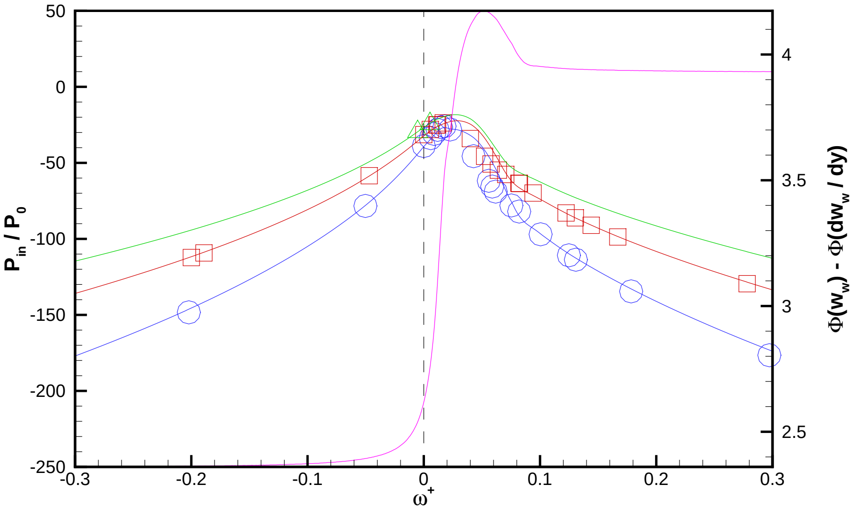

FIG. 12. Input Power P_{in} versus wave frequency ω^+ at various Re at $A^+ = 12$ and $\lambda^+ = 1250$. Open symbols and colors as in figure 7. Lines are the laminar solution at $Re_\tau = 200$ (blue), $Re_\tau = 1000$ (red) and $Re_\tau = 2000$ (green). The magenta line is the phase lag between the spanwise wall velocity w_w and its derivative $\mathrm{d}w/\mathrm{d}y$ from the laminar solution.

on low-Re observations but it is useful as a benchmark in this range of Re, even though other choices have been proposed or can be thought, an example[2] is $\mathrm{R} = \alpha + Re_\tau^\beta$, where β is eventually $\beta(Re)$.

It is clear from the present study that the sensitivity coefficient γ is not unique. In the case of oscillating wall ($\kappa_x = 0$), the empirical coefficient $\gamma \approx -0.20$ is confirmed for the maximum drag reduction R_{max}. The slightly higher value of $\gamma = -0.25$ is achieved at constant $T^+ = 100$ because the optimal period is shortening with Re. On the other hand, drag reduction ratios at short periods of forcing, for example corresponding to $\omega^+ = 0.2$ are less sensitive to a change in Re, leading to $\gamma \approx -0.08$.

If we extend to the traveling waves, the scenario is unexpectedly rich. The drag reduction ridge is reduced in size and looses its low-frequency low-wavenumber tail, where we locally measure a high sensitivity of $\gamma = -0.25$. The trend suggests that this part of the drag reduction ridge is a low-Re effect, that is deemed to disappear quickly with Re. The high-wavenumber high-frequency part is instead less sensitive ans shows a $\gamma = -0.08$ at ($\omega^+ = 0.04$, $\kappa_x^+ = 0.015$) which reduces to $\gamma = -0.07$ at ($\omega^+ = 0.08$, $\kappa_x^+ = 0.035$). This observation is of great importance since the upper part of the ridge is still a region of high drag reduction ratios, ranging between 0.4 and 0.5, suggesting the possibility to preserve significant value of R at high Re. Surprising is also the behavior of the DI region: its intensity is reduced while its extension seems to widen and influence the neighborhood. At $Re_\tau = 1000$ the drag increase almost disappears or turns to very little DR. In the latter case a sensitivity exponent can not even be defined within the framework of the $\mathrm{R} \sim Re_\tau^\gamma$ law and around ($\omega^+ = 0.06$, $\kappa_x^+ = 0.005$) goes from 3 to ∞. Finally we observe that at high frequencies ($|\omega^+| = 0.2$) both forward- and backward-traveling waves are not strongly affected by a change of Re: γ is -0.08 at low wavenumbers and decreases further to -0.05 at $\kappa_x^+ = 0.04$.

To summarize, the Re-effect is proved to be lower at higher wavenumbers and at increasing distances from the DI region, whose influence increases with Re, though its intensity reduces. This implies that on the left of the DI valley the more insensitive regions move towards lesser frequencies, even negative when necessary, and higher wavenumbers, while the opposite occurs to the other side. As a consequence, the optimal set of control parameters is not constant with Re.

IV. INPUT POWER AND POWER BUDGET

From figure 12 one sees first that the laminar GSL solution predicts the input power rather well, but regions of the parameter space exist where prediction is not perfect. In particular when the equivalent period, defined by Quadrio et al[28] as $\mathcal{T}^+ = \lambda_x^+/(\mathcal{U}_w^+ - c^+)$ is about ten. $\mathcal{U}_w$ is the convective speed of

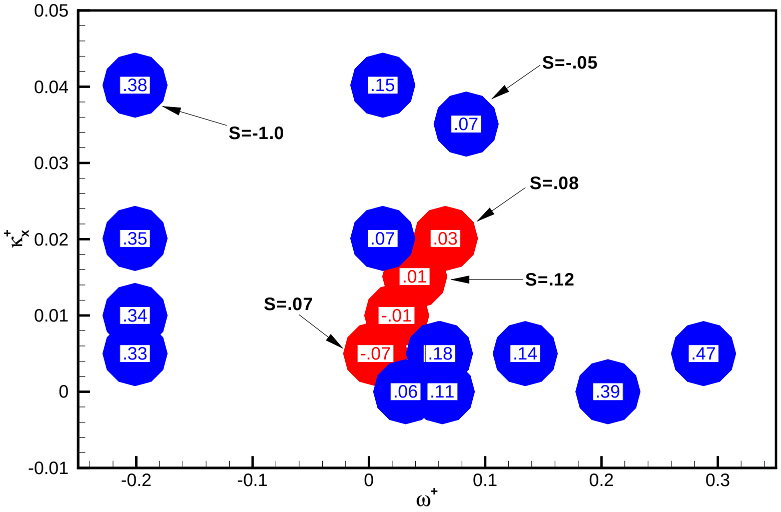

FIG. 13. Map of the change $\Delta S = S(Re_\tau = 1000) - S(Re_\tau = 200)$ in the net power budget S: in the circle the value ΔS. Arrows points the value of S at $Re_\tau = 1000$. Blue circles: negative S; Red circles: positive S.

the skin-friction information, as defined in Quadrio & Luchini[26] . In this region, the traveling-wave is seen as standing by the near-wall turbulent structures with which shares the same velocity, leading to a lock-in effect that leads to drag increase and deviations from the laminar solution of the generalized Stokes layer.The second, most important observation is that P_{in}/P_0, that is the percentage of the pumping power required to run the flow, slightly decreases for increasing Re. Another way of putting it is that P_{in} is constant when expressed in inner units. This was suggested by Ricco & Quadrio[30], can be verified through a nondimensionalization of the laminar expression of P_{in} and is fully confirmed here. Whenever the laminar solution holds, the input power is seen to decrease as $Re_\tau^{-0.136}$. This opens up interesting perspective as far as the net energy saving S is concerned: in several parts of the control parameter space P_{in}/P_0 decreases faster R, meaning that S could even increase with Re. Evidence is given in figure 13, where the change ΔS in net power budget when Re_τ is increased from 200 to 1000 is represented. At these A^+ most of the parameter space at $Re_\tau = 1000$ still has $S < 0$ (blue circles), though rapidly increasing and sometimes even approaching positive values. For control parameters lying on the low-wavenumber tail of the DR ridge S is positive (red circle) but showed a decrease of 7%. Here R decreases faster than P_{in}/P_0. On the upper part of the ridge the trend is opposite, a positive and increasing S is achieved. This result is encouraging especially if we consider that much lower A^+ should be considered when interest is focused on the net power budget.

V. CONCLUDING DISCUSSION

The main messages conveyed by the results presented so far is that the general picture, as it stands today, of how the drag reduction ability of techniques based on spanwise forcing decreases as Re increases might need to be revised. Our data indicate first of all that that drag reduction decrease with Re at a rate which depends strongly on the region of the parameters space. Therefore, the optimal set of control parameters changes with Re and new regions of the parameter space may lead to interesting values of drag reduction and net power saving, meaning that a meaningful parametric study has to span a large portion of parameters space and not only focus on the neighborhood of the low-Re optimum.

A possible scenario is shown in figure 15. The optimal control parameters shift towards higher wavenumbers and away from the drag increase region, whose intensity strongly reduces with Re, while the portion of parameter space affected by its influence seems to increase. The Re-effect appears to both reduce drag reduction and widen the DI region of influence, suggesting that two still unknown different mechanisms exists through which the Re-effect acts.

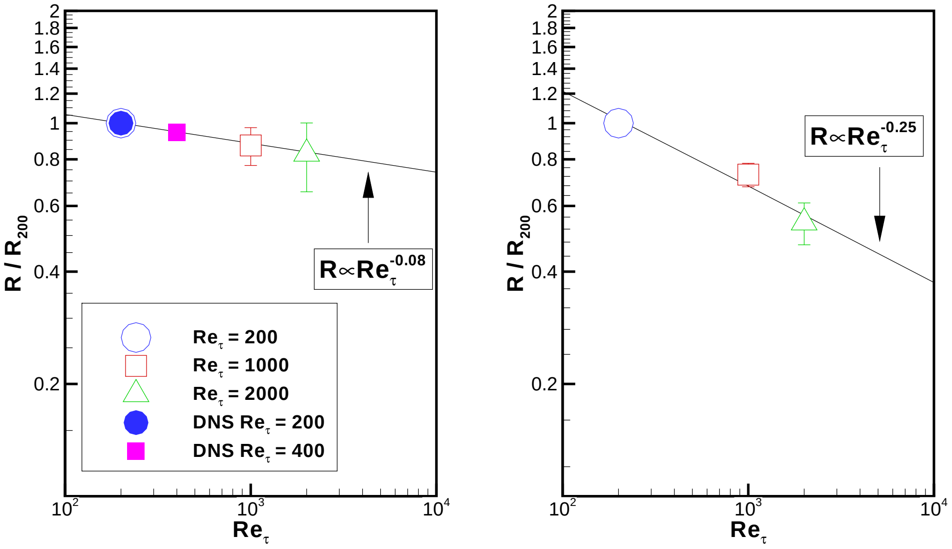

FIG. 14. Relative change in R as function of Re_τ for traveling waves with wavenumber $\kappa_x^+ = 0.005$. On the left $\omega^+ = -0.2$, on the right $\omega^+ = 0.005$. Both results with the reduced channel and bespoke fullchannel simulations are represented.

The power law $R \sim Re_\tau^\alpha$ traditionally used to quantify the Re-effect may be too simple a law to clearly depict the complex scenario and clearly fails in cases where the drag increase (R¡0) turns to drag reduction (R¿0).

We are well aware of the limitations implicit in the present study, which in particular has its weakest spot in the rather limited size of the computational domain. Although first-order effects can be ruled out, since the domain is always many many times larger than the MFU, the present results should be considered as suggestive only, though predictions quantitatively agree with simulations of Touber & Leschziner[33]. Moreover, they are in line with other full-DNS data recently obtained by Hurst, Chung & Lockerby[13].

On the other hand, if our simplified framework well represents the drag reduction, it would imply that large scale motions only marginally participate in the mechanisms behind the Re-effect which indeed would be due to near-wall dynamics. This scenario is even more interesting considered that dynamical importance of linear phenomena in the near-wall region, giving hope for simplified representations of drag reducing mechanisms and confirming the studies of Duque et al.[10].

[1] F. Auteri, A. Baron, M. Belan, G. Campanardi, and M. Quadrio. Experimental assessment of drag reduction by traveling waves in a turbulent pipe flow. *Phys. Fluids*, 22(11):115103/14, 2010.

[2] M. Belan and M. Quadrio. A perturbative model for predicting the high-Re behaviour of turbulent drag reduction techniques. *Submitted to ZAMM.*, 2013.

[3] T. W. Berger, J. Kim, C. Lee, and J. Lim. Turbulent boundary layer control utilizing the Lorentz force. *Phys. Fluids*, 12(3):631–649, 2000.

[4] J.-I. Choi, C.-X. Xu, and H. J. Sung. Drag reduction by spanwise wall oscillation in wall-bounded turbulent flows. *AIAA J.*, 40(5):842–850, 2002.

[5] K-S. Choi, J.R. DeBisschop, and B.R. Clayton. Turbulent boundary-layer control by means of spanwise-wall oscillation. *AIAA J.*, 36(7):1157–1162, 1998.

[6] K-S. Choi and M. Graham. Drag reduction of turbulent pipe flows by circular-wall oscillation. *Phys. Fluids*, 10(1):7–9, 1998.

[7] R.B. Dean. Reynolds number dependence of skin friction and other bulk flow variables in two-dimensional rectangular duct flow. *Trans. ASME I: J. Fluids Eng.*, 100:215, 1978.

[8] Y. Du and G. E. Karniadakis. Suppressing wall turbulence by means of a transverse traveling wave. *Science*, 288:1230–1234, 2000.

[9] Y. Du, V. Symeonidis, and G. E. Karniadakis. Drag reduction in wall-bounded turbulence via a transverse travelling wave. *J. Fluid Mech.*, 457:1–34, 2002.

[10] C.A. Duque-Daza, M.F. Baig, D.A. Lockerby, S.I. Chernyshenko, and C. Davies. Modelling turbulent skin-friction control using linearised Navier-Stokes equations. *J. Fluid Mech.*, 702:403–414, 2012.

[11] O. Flores and J. Jiménez. Hierarchy of minimal flow units in the logarithmic layer. *Phys. Fluids*, 22(7):071704, 2010.

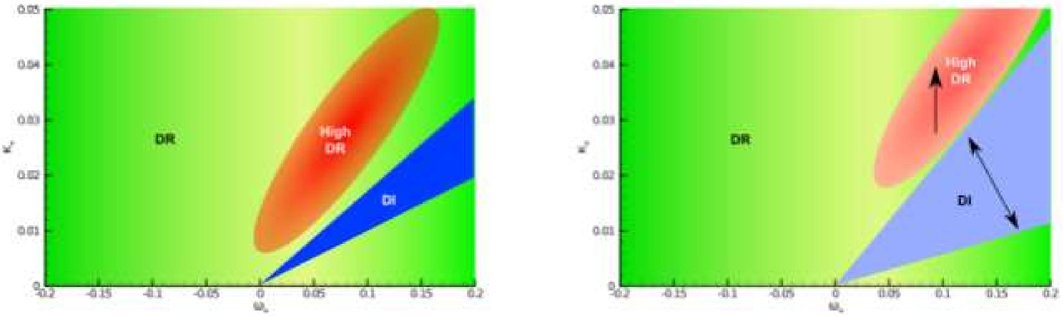

FIG. 15. A qualitative schematic of the changes in drag reduction with Re. Drag reduction decreases from red to green. In blue regions of drag increase, while in white regions where the control has low effect.

[12] R. Garcia-Mayoral and J. Jiménez. Hydrodynamic stability and the breakdown of the viscous regime over riblets. *J. Fluid. Mech.*, 678:317–347, 2011.

[13] E. Hurst, Y. M. Chung, and D. A. Lockerby. The Reynolds number effect of turbulent drag reduction. In *EUROMECH Fluid Mechanics Conference -9 (EFMC9), Rome, Italy*, 2013.

[14] K. Iwamoto, K. Fukagata, N. Kasagi, and Y. Suzuki. Friction drag reduction achievable with near-wall manipulation at high Reynolds numbers. *Phys. Fluids*, 17(011702):4, 2005.

[15] J. Jiménez. Computing high-Reynolds-number turbulence: will simulations ever replace experiments? *J. Turbulence*, 4:22, 2003.

[16] J. Jiménez and P. Moin. The minimal flow unit in near-wall turbulence. *J. Fluid Mech.*, 225:213–240, 1991.

[17] J. Jiménez and A. Pinelli. The autonomous cycle of near-wall turbulence. *J. Fluid Mech.*, 389:335–359, 1999.

[18] W.J. Jung, N. Mangiavacchi, and R. Akhavan. Suppression of turbulence in wall-bounded flows by high-frequency spanwise oscillations. *Phys. Fluids A*, 4 (8):1605–1607, 1992.

[19] N. Kasagi, Y. Hasegawa, and K. Fukagata. Towards cost-effective control of wall turbulence for skin-friction drag reduction. volume 132 of *Advances in Turbulence XII*, pages 189–200. Springer, 2009.

[20] J. Kim and T.R. Bewley. A linear systems approach to flow control. *Annu. Rev. Fluid Mech.*, 39:383–417, 2007.

[21] M. Leschziner, H. Choi, and K.-S. Choi. Flow control approaches in aerodynamics: progress and prospects. *Phil. Trans. R. Soc. A*, 369(1940):1349–1351, 2011.

[22] P. Luchini and M. Quadrio. A low-cost parallel implementation of direct numerical simulation of wall turbulence. *J. Comp. Phys.*, 211(2):551–571, 2006.

[23] R. Moarref and M. R. Jovanović. Model-based design of transverse wall oscillations for turbulent drag reduction. *J. Fluid Mech.*, 707:205–240, 2012.

[24] N. V. Nikitin. On the mechanism of turbulence suppression by spanwise surface oscillations. *Fluid Dyn.*, 35(2):185–190, 2000.

[25] J. Pang and K.-S. Choi. Turbulent drag reduction by Lorentz force oscillation. *Phys. Fluids*, 16(5):L35–L38, 2004.

[26] M. Quadrio and P. Luchini. Integral time-space scales in turbulent wall flows. *Phys. Fluids*, 15(8):2219–2227, 2003.

[27] M. Quadrio and P. Ricco. Critical assessment of turbulent drag reduction through spanwise wall oscillation. *J. Fluid Mech.*, 521:251–271, 2004.

[28] M. Quadrio, P. Ricco, and C. Viotti. Streamwise-traveling waves of spanwise wall velocity for turbulent drag reduction. *J. Fluid Mech.*, 627:161–178, 2009.

[29] M. Quadrio and S. Sibilla. Numerical simulation of turbulent flow in a pipe oscillating around its axis. *J. Fluid Mech.*, 424:217–241, 2000.

[30] P. Ricco and M. Quadrio. Wall-oscillation conditions for drag reduction in turbulent channel flow. *Intl J. Heat Fluid Flow*, 29:601–612, 2008.

[31] P. Ricco and S. Wu. On the effects of lateral wall oscillations on a turbulent boundary layer. *Exp. Therm. Fluid Sci.*, 29(1):41–52, 2004.

[32] S. Tamano and M. Itoh. Drag reduction in turbulent boundary layers by spanwise traveling waves with wall deformation. *J. Turbulence*, 13:XXX, 2012.

[33] E. Touber and M.A. Leschziner. Near-wall streak modification by spanwise oscillatory wall motion and drag-reduction mechanisms. *J. Fluid Mech.*, 693:150–200, 2012.

[34] S.M. Trujillo, D.G. Bogard, and K.S. Ball. Turbulent Boundary Layer Drag Reduction using an Oscillating Wall. *AIAA Paper 97-1870*, 1997.